spectrum of the CW direction is due to a small reflection of light from the CCW pulse train. We verified this by removing GSAM2 to suppress CCW lasing and noted that this peak disappeared. The peak-to-pedestal ratio of the RF spectrum for CW-propagating pulses was ~75 dB, implying good mode-locking stability [26]. A lower ratio of ~50 dB was observed for the CCW direction, suggesting that this mode-locked pulse train is slightly noisier, which could be related to the different sub-paths in CW and CCW directions and the order of components experienced by light in the cavity, in addition to the different output powers.

The pulse shapes were investigated using an autocorrelator and the corresponding traces together with a sech^2 fit are reported in Figs. 3(c) and 3(d). The corresponding pulse durations of the CW and CCW pulses were ~750 fs and ~850 fs, respectively. The time-bandwidth products (TBP) of the counter-circulating pulses were calculated as 0.39 and 0.34, indicating that the output pulses were nearly transform-limited soliton pulses. As depicted in the insets of Figs. 3(c) and 3(d), the fundamental repetition rates for counter-circulating mode-locked pulses were not identical because of their distinct cavity lengths. The corresponding repetition rates for CW and CCW directions were measured as ~7.68 MHz and ~6.90 MHz. By observing the pulse trains over a long range, we notice only very minimal Q-switching instabilities in the mode-locking regime. Q-switching instabilities can arise due to interplay between saturation effects in the SA, and the gain medium favoring higher pulse energies with lower round trip losses [27]. We believe the slight instability we observe is due to the low modulation depth (~2%) and high non-saturable loss (~40%) of the SA, which is a cause of the noise we observe in the optical and RF spectra. Fabrication of a graphene SA with higher modulation depth is expected to reduce this instability and improve mode-locking performance. We also expect our cavity design will enable bidirectional mode-locking at other wavelengths if appropriate gain fiber and couplers are used, since graphene is an ultra-wideband SA.

Under an incident pump power of 150 mW, the average output power for the CW and CCW directions was 180 μW and 400 μW, respectively. The calculated pulse energy was 23.5 pJ and 58 pJ, respectively. Asymmetry of the laser cavity is the reason behind the different average output powers.

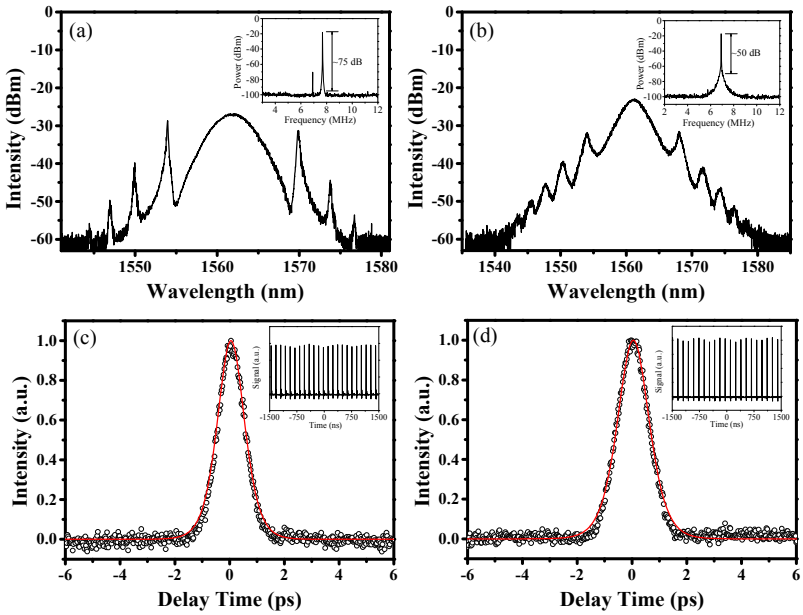

Fig. 4. Bidirectional pumping: Output optical spectrum of the CW pulses (a) and the CCW pulses (b). Insets are the corresponding RF spectra. Autocorrelation traces of the CW pulses (c) and the CCW pulses (d). Insets are the oscilloscope traces.

#200736 - $15.00 USD Received 5 Nov 2013; revised 9 Jan 2014; accepted 9 Jan 2014; published 20 Feb 2014

Subsequently, we used bidirectional pumping by using both WDMs. Similar to unidirectional pumping, mode-locking of the laser self-started in CCW direction at a pump power of ~200 mW (with forward pump power of 120 mW and backward pump power of 80 mW). In order to initiate simultaneous mode-locking, careful adjustment of PC1, PC2 and PC3 was required. At first, multiple pulses were observed in each round-trip of the cavity, then by reducing the pump power to 175 mW (with forward pump power reducing to 95 mW and the backward pump power reducing to 80 mW) we were able to achieve fundamentally mode-locked single pulse soliton operation in both directions. Once simultaneously mode-locked, the laser would remain stable for hours.

The output optical spectra of the simultaneously generated CW and CCW light pulses are shown in Figs. 4(a) and 4(b). The central wavelengths of the CW and CCW pulses were located at 1561.9 nm and 1561.1 nm, respectively. The FWHM spectral bandwidth for the CW direction was 4.4 nm and 3.4 nm for the CCW direction. The counter-circulating pulses exhibit spectral sidebands, which clearly indicate soliton pulse shaping. The RF spectrum of laser is shown in the inset of Figs. 4(a) and 4(b), indicating a repetition rate of ~7.68 MHz for CW-propagating light and ~6.90 MHz for the CCW pulse train. The measured peak-to-pedestal ratio for the CW and CCW directions was ~75 dB and ~50 dB, respectively.

Figures 4(c) and 4(d) illustrate the measured autocorrelation traces for both directions including a sech^2 fit, which indicates a width of ~750 fs and ~880 fs for CW and CCW pulses respectively. Taking into account spectral bandwidths, the TBP of the laser is equal to 0.41 and 0.37, which is close to the transform limit for sech^2-shaped laser pulses. Insets of Figs. 4(c) and 4(d) show the measured oscilloscope trace of the output mode-locked pulses. The counter-circulating pulses operate at a period of 130 ns and 145 ns. The average output power of CW and CCW soliton pulses was about 200 μW and 430 μW, corresponding to pulse energies of 26 pJ and 62 pJ.

The mode-locked pulse train characteristics are very similar for our laser when using either a unidirectional or bidirectional pump scheme. This shows that despite the bidirectional propagation of pulses in our laser cavity, the choice of pumping a single end of the gain medium or pumping both ends does not have a significant effect on the performance of our laser.

5. Conclusion

In conclusion, we have reported a graphene-based passively mode-locked bidirectional fiber laser. Two counter-circulating trains of soliton pulses with distinct output characteristics were generated simultaneously. This was achieved by appropriately adjusting the cavity birefringence and introducing controllable losses through the combination of a fast-axis blocking PM circulator and PC. The unique features offered by bidirectional mode-locked fiber lasers, along with the easy graphene SA preparation pave the way to dual ultrafast light sources in a single simple low-cost cavity.

Acknowledgments

The authors would like to acknowledge Dr. K. Wu for providing the fiber mirrors. This work was partially supported by Academic Research Fund Tier 1 Grant (RG22/10) of Ministry of Education and Nanyang Technological University, Singapore.

#200736 - $15.00 USD Received 5 Nov 2013; revised 9 Jan 2014; accepted 9 Jan 2014; published 20 Feb 2014